


ORIGINAL RESEARCH ARTICLE

Castration-induced prostate epithelial cell apoptosis results from targeted oxidative stress attack of M1₁₄₂-macrophages

Guilherme O. Barbosa^{1*} | Juliete A. F. Silva^{1*} | Aline Siqueira-Berti¹ | Umar Nishan^{1*} |
 Rafaela Rosa-Ribeiro¹ | Silvia B. P. Oliveira¹ | Mariana O. Baratti^{1,2} |
 Danilo Ferrucci¹ | Julio C. O. Santana¹ | Danilo M. Damas-Souza¹ |
 Alexandre Bruni-Cardoso³ | Taize M. Augusto⁴ | Felipe Corrêa-da-Silva⁵ |
 Pedro M. Moraes-Vieira⁵ | Dagmar R. Stach-Machado¹ | Sergio L. Felisbino^{2,6} |
 Gustavo B. Menezes⁷ | Carlos L. Cesar^{2,8} | Hernandes F. Carvalho^{1,2} 

¹Department of Structural and Functional Biology, State University of Campinas, Campinas, São Paulo, Brazil

²National Institute for Science and Technology of Photonics Applied to Cell Biology (INFABIC), Campinas, São Paulo, Brazil

³Department of Biochemistry, University of São Paulo, São Paulo, São Paulo, Brazil

⁴Department of Pathology, Jundiaí Medical School, Jundiaí, São Paulo, Brazil

⁵Department of Genetics, Evolution, Microbiology, and Immunology, State University of Campinas, Campinas, São Paulo, Brazil

⁶Department of Morphology, São Paulo State University, Botucatu, São Paulo, Brazil

⁷Department of Morphology, Federal University of Minas Gerais, Belo Horizonte, Minas Gerais, Brazil

⁸Department of Quantum Electronics, State University of Campinas, Campinas, São Paulo, Brazil

Correspondence

Hernandes F. Carvalho, Department of Structural and Functional Biology, State University of Campinas, Rua Charles Darwin s/n, Bld N, Rooms 10/11, Campinas, São Paulo 13083-863, Brazil.
 Email: hern@unicamp.br

Funding information

Conselho Nacional de Desenvolvimento Científico e Tecnológico; Fundação de Amparo à Pesquisa do Estado de São Paulo, Grant/Award Number: 2009/16150-6; FAPESP; CNPq

Present address

[†]Umar Nishan Department of Chemistry, Kohat University of Science and Technology, Kohat, Pakistan.

Abstract

Prostate development and function are regulated by androgens. Epithelial cell apoptosis in response to androgen deprivation is caspase-9-dependent and peaks at Day 3 after castration. However, isolated epithelial cells survive in the absence of androgens. *Znf142* showed an on-off expression pattern in intraepithelial CD68-positive macrophages, with the on-phase at Day 3 after castration. Rats treated with gadolinium chloride to deplete macrophages showed a significant drop in apoptosis, suggesting a causal relationship between macrophages and epithelial cell apoptosis. Intraepithelial M1-polarization was also limited to Day 3, and the inducible nitric oxide synthase (iNOS) knockout mice showed significantly less apoptosis than wild-type controls. The epithelial cells showed focal DNA double-strand breaks (DSB), 8-oxoguanine, and protein tyrosine-nitrosylation, fingerprints of exposure to peroxynitrite. Cultured epithelial cells induced M1-polarization and showed focal DSB and underwent apoptosis. The same phenomena were reproduced in LNCaP cells cocultured with Raw 264.7 macrophages. In conclusion, the M1₁₄₂-macrophage (named after *Znf142*) attack causes activation of the intrinsic apoptosis pathway in epithelial cells after castration.

KEYWORDS

apoptosis, castration, epithelial cells, macrophage, prostate

*These authors have contributed equally to this work.

1 | INTRODUCTION

Prostate epithelial cell death after castration is a classical example of apoptosis (Kerr & Searle, 1973) and is considered as a direct response to the falling androgen levels. It has been determined that the circulating and tissue testosterone and dihydrotestosterone (DHT) fall to undetectable levels within 24 hr after castration (Kashiwagi et al., 2005), and that endothelial cells die as earlier as 24 hr after castration (Shabsigh et al., 1998). However, rodent models show a peak of apoptosis only 3 days after castration (Damas-Souza, Oliveira, & Carvalho, 2010; English, Kyrianiou, & Isaacs, 1989; Isaacs, 1984; Kyrianiou & Isaacs, 1988).

Intriguingly, isolated prostate epithelial cells do not undergo apoptosis in response to androgen deprivation. Kurita et al. (2001) used tissue recombinants and the testicular feminization mouse defective in the response to androgens due to an inactivating mutation in the androgen receptor gene and showed that epithelial cell apoptosis does not require the androgen receptor in the epithelial cells to undergo apoptosis in response to castration. They suggested that apoptosis would be triggered by unknown stroma-derived factors. However, if the interaction of a soluble factor with any death receptor at the cell surface were responsible for triggering apoptosis, epithelial cell death resulting from androgen deprivation would rely on the extrinsic apoptosis pathway and caspase-8 activation. However, castration-induced apoptosis in the prostate epithelium is associated with caspase-9 activation (McPherson et al., 2010; Rosa-Ribeiro, Barbosa, Kühne, & Carvalho, 2014), suggesting that the intrinsic pathway is activated. In fact, despite existing evidence showing that FAS-L, released from the extracellular matrix by matrilysin (Powell, Fingleton, Wilson, Boothby, & Matrisian, 1999), contributes to the bulk of apoptosis occurring 72 hr after castration, the FAS-L/FAS pathway contribution to prostate epithelial cell death has been ruled out (Davis, Nastiuk, & Krolewski, 2011; Sugihara et al., 2001). One of these studies (Davis et al., 2011) has also excluded tumor necrosis factor (TNF)-related apoptosis-inducing ligand (TRAIL) and, while pinpointing a dependence on tumor necrosis factor (TNF), has shown that soluble TNF is not capable of inducing apoptosis in noncastrated animals (Davis et al., 2011).

Prostate adenocarcinoma (PCa) is the second leading cause of human male death to cancer. It will reach one in eight men (12% incidence) and virtually all men at the age of 85. It is assumed as a slowly progressing disease. Castration-resistant prostate cancer (CRPC) arises after orchiectomy or chemical castration used to treat advanced prostate cancer. However, PCa and CRPC are quite distinct diseases, differing with respect to androgen-dependence, growth rate, and aggressiveness. Given that CRPC grows under low androgen levels, most of the behavior exhibited by CRPC has been imputed to modifications in the androgen receptor, which is assumed to be responsible for the cell's ability to proliferate under exquisitely low levels of androgens (Feldman & Feldman, 2001; Heinlein & Chang, 2004), leading to positive selection.

Expression and activation of a series of inflammatory response-associated transcription factors (Desai et al., 2004; Rosa-Ribeiro &

Nishanet et al., 2014), the influx of immune cells, and altered levels of cytokines (Desai et al., 2004) are relevant aspects of changes taking place in the hypoandrogen environment. Recently, we have demonstrated that a subset of macrophages is recruited to the epithelial layer and perform the clearance of epithelial cell corpses. These macrophages express autophagy antigens and preserve a noninflammatory environment. Blockade of autophagy resulted in overt inflammation of the prostate gland (Silva et al., 2018). These diverse functions depend on poorly understood, complex gene expression networks and cell-cell interactions. Accordingly, we have found that some genes escape the simplistic on-or-off expression pattern of androgen-regulation via the androgen receptor (Rosa-Ribeiro & Nishan et al., 2014).

ZNF142 is a protein-coding gene located in chromosome 2q35. This gene was first described among 15 other zinc finger-encoding complementary DNAs (cDNAs) with potential implications in human diseases (Tommerup & Vissing, 1995). The predicted protein coded by transcript variant 1 has 1,687 amino acids (estimated molecular mass 168.7 kDa), and belong to the Kruppel family of zinc finger proteins, with 31 C2H2-type zinc fingers. Given these structural aspects, ZNF142 is a putative DNA-binding transcription regulator.

In this study, we show that coincident *Znf142* expression and M1-macrophage polarization are mechanistically linked to epithelial cell death via targeted oxidative stress and activation of epithelial cell apoptosis after castration.

2 | METHODS

2.1 | Ethical approval

The experimental design, including sample size and procedures, were approved by the State University of Campinas Committee on the Use of Experimental Animals, according to the Brazilian College for Animal Experimentation, under protocol nr. 1490-1.

2.2 | Animals

Thirty-seven 90-day-old Wistar male rats were used in this study. Animals were sham-operated ($n = 3$), and maintained as controls, or castrated ($n = 24$) under anesthesia with 80 mg/kg body weight ketamine hydrochloride and 10 mg/kg body weight xylazine hydrochloride and assigned to seven groups, which were killed daily (Day 1 through 7 after castration) by anesthetic overdose. Three animals were killed at each time point, except on Day 3 ($n = 6$), as three animals were used for transmission electron microscopy. The ventral prostates (VPs) were then immediately dissected, freed of adherent tissue, and fixed for TEM, paraffin embedding or snap frozen in liquid nitrogen for biochemical analysis. Six Wistar male rats were treated with gadolinium chloride (10 mg/kg body weight), according to Liou et al. (2013), 24 hr before surgery. Animals were then castrated ($n = 3$) or sham-operated ($n = 3$) and the VP collected and processed for histology, immunohistochemistry for the identification of macrophages (Silva et al., 2018) and terminal deoxynucleotidyl transferase dUTP nick end labeling (TUNEL) reaction

72 hr later. Ten iNOS knockout (KO) mice and 10 C57Bl/6 mice were sham-operated ($n = 5$) or castrated ($n = 5$) as above and the VP collected for histology and TUNEL reaction 72 hr after surgery.

Five Transgenic mice, expressing the soluble green fluorescent protein (GFP) under the actin promoter, and five transgenic mice, expressing the Ds-Red Express fluorescent protein under the ubiquitin-promoter, were used for isolation of prostate epithelial cells and bone marrow mononuclear precursors, respectively.

2.3 | Transmission electron microscopy

The material was processed using routine procedures (Carvalho & Line, 1996). In brief, the small fragments (1 mm^3) were fixed for 24 hr in Karnovsky fixative, postfixed in 1% osmium tetroxide for 2 hr, and dehydrated in a graded acetone series before embedding in Araldite 502 (Electron Microscopy Science, Hatfield, PA). Ultrathin sections (50–70 nm) were cut with a diamond knife and contrasted with uranyl acetate and lead citrate. The specimens were observed and documented under a Jeol 1010 transmission electron microscope.

2.4 | Quantitative real-time RT-PCR (qRT-PCR)

Ventral prostates were dissected under RNase free conditions. Thirty milligrams of the tissue was used for total RNA extraction. Subsequently, the tissue fragments were extracted using Illustra RNAspin Mini Kits (GE Healthcare, Marlborough, MA), according to manufacturer's instructions. RNA purity was analyzed by the absorbance ratio 260/280 (values higher than 1.8) and by electrophoresis in 1.2% agarose gel under denaturing conditions. The RNA concentration in each sample was determined in an Ultraspec 2100 pro spectrophotometer (GE Life Sciences, Chicago, IL). Five micrograms of total RNA was reverse-transcribed with 200 U SuperScript III (Invitrogen, Carlsbad, CA) and oligo (dT)12–18 primer (Invitrogen), according to manufacturer's instructions. cDNA was quantified by spectrophotometry.

qRT-PCR was performed, using TaqMan Universal PCR Master Mix (Applied Biosystems, Foster City, CA) in the Applied Biosystems 7300. Inventoried primers (forward: GGTGGTCACTGGAGATT-CAGTCA, reverse: GGCTTGGACTAAACCATTGATTTTC) and the FAM-conjugated probe (AGGTCAAACCATACACTAC) were purchased from Applied Biosystems. cDNA (20 ng) was used in each reaction according to universal cycling conditions for the TaqMan system. The results were normalized using the C_t (threshold cycle) values of the internal control glyceraldehyde-3-phosphate dehydrogenase (GAPDH) on the same plates. GAPDH was chosen as an internal control because it was found to show the least standard deviation among the experimental groups after testing nine others for this specific purpose. The equation $\Delta C_t = C_t$ (target gene) – C_t (internal control) was used for normalization of the results. To quantify and acquire the fold-change variation of our genes, the mathematical model $2^{-\Delta\Delta C_t}$ was utilized. Our genes and GAPDH assays had their efficiency calculated through the equation: $E = 10(-1/\text{slope})$. All reactions were performed in technical triplicates and the experiment was repeated twice.

2.5 | Cell isolation and coculturing

The VP was dissected out male C57BL/6- or GFP-mice under sterile conditions and immersed in disinfection by-products solution (DBPS), containing 5% penicillin/streptomycin, and chopped in small fragments with a razor blade. The fragments were transferred to RPMI, containing 1 mg/ml collagenase I, and incubated for 3 hr at 3°C. The resulting suspension was filtered through sterile gauze to retain large fragments and the cell suspension centrifuged to collect the isolated cells. The pellet was suspended in 5 ml of RPMI and fractioned on a Percoll gradient. The upper cell fraction containing stromal cells was discarded and the lower cell fraction containing the epithelial cells collected and transferred to fresh RPMI medium, containing 10% fetal calf serum. Cells were used as first passage and the medium changed to remove serum and to add (or not) 1 nM DHT (Sigma-Aldrich, Saint Louis, MO), before coculturing with isolated macrophages or undifferentiated bone marrow mononuclear precursors.

Bone marrow cells were washed off the DsRed-mouse femur with phosphate buffered saline. The cell suspension was diluted 20× in 2% acetic acid solution and the concentration adjusted to 2×10^6 cells/ml and cultured in RPMI containing 10% fetal calf serum and 10 ng/ml M-CSF for 24 hr to select granulocytes/monocytes before used in the cocultures with the epithelial cells.

For coculturing, the mononuclear cells were added on top of the isolated epithelial cells at different proportions. A final 50 mononuclear cells per epithelial cell proportion was used for better imaging. We first used iNOS-positive, M1-macrophages differentiated by treatment with bacterial lipopolysaccharide (LPS) and interferon-gamma before coculturing, and then used the undifferentiated mononuclear precursor cells.

Raw 264.7 cells (mouse monocytes/macrophages) were cultured in high glucose Dulbecco's modified Eagle medium (DMEM) plus 10% fetal calf serum and 1% antibiotics. LNCap (lymph node carcinoma of the prostate) cells were cultured according to the ATCC instructions. Cocultures were done in half-to-half mixtures of the conditioned medium in the presence or absence of androgen stimulus (10 nM R1881).

2.6 | TUNEL reaction

TUNEL reaction was done to detect DNA double-strand breaks (DSB), using the in situ cell death detection kit, fluorescein (Roche Applied Science, Pleasanton, CA). TUNEL-positive cells were counted in at least 10 microscopic fields (×40 objective) picked at random per animal.

2.7 | Immunohistochemistry

Paraformaldehyde (PFA)-fixed, paraffin-embedded tissues were cut into 5- μm sections, mounted on silane-treated slides, dewaxed in xylene, and rehydrated. The sections were briefly treated in a microwave oven in 10 mM citrate buffer pH 6.0. The sections were blocked with 3% hydrogen peroxide for 10 min, followed by incubation with 5% bovine serum albumin for 1 hr. The sections were incubated overnight with antibodies against ZNF142 (cat no. 11195; Abcam, Cambridge, MA or cat

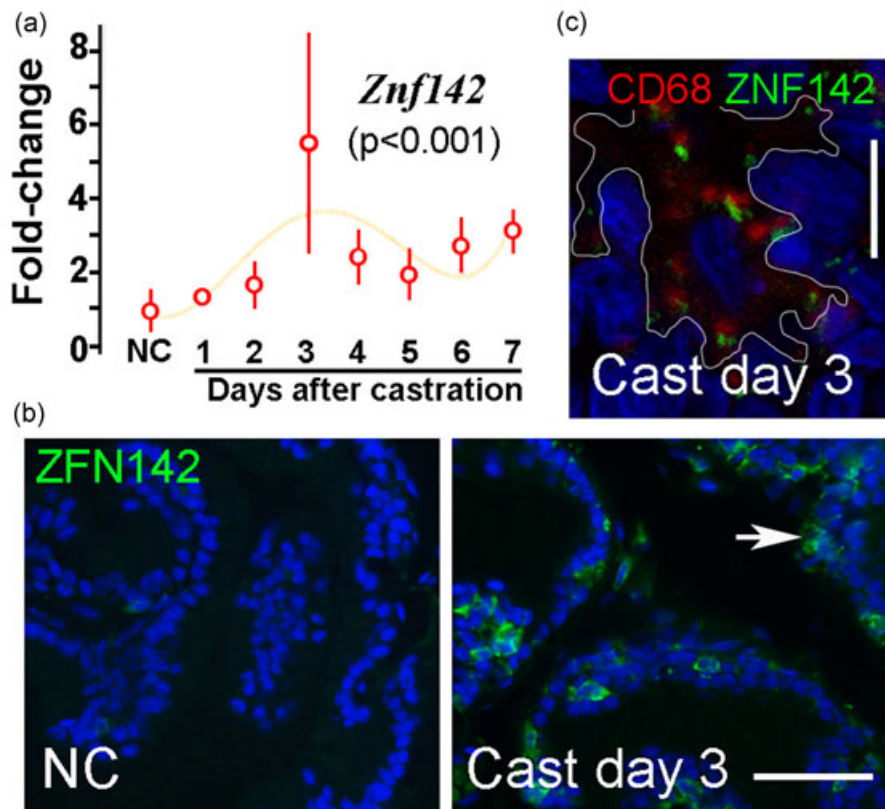


FIGURE 1 *Znf142* is transiently expressed in the rat VP at Day 3 after castration and identifies a subpopulation of intraepithelial macrophages. (a) Quantitative real-time RT-PCR demonstrated a significant increase in *Znf142* messenger RNA 72 hr after castration. (b) ZNF142-positive cells were found in the epithelial layer 72 hr after castration, but not in sham-castrated controls. Scale bar = 100 μm . (c) ZNF142-positive cells were identified as macrophages by double staining with CD68. ZNF142 and CD68 label distinct structures within the cells. Scale bar = 5 μm [Color figure can be viewed at wileyonlinelibrary.com]

no. 8540; Cell Signaling Technology, Danvers, MA), CD68 (ED1; cat no. MAB1435; Millipore, Billerica, MA), 8-oxoguanine (cat no. ab206461; Abcam) or nitrotyrosine (cat no. ab742789; Abcam), iNOS (cat no. 15223; Abcam), cleaved caspase-9 (cat no. 95075; Cell Signaling Technology), cleaved caspase-8 (cat no. 94295; Cell Signaling Technology).

The primary antibody was detected with proper Alexafluor-conjugated secondary antibodies (Invitrogen). Cultured cells grown on coverslips were fixed with cold methanol and subjected to immunohistochemistry, as above. Negative controls were obtained by omitting the primary antibody step. Sections were counterstained with 4',6-diamidino-2-phenylindole (DAPI) and examined under a Zeiss LSM780 confocal microscope (at INFABiC).

2.8 | Intravital microscopy

Intravital microscopy was an adaptation to the ventral prostate of the previously published protocol, used for the liver (Marques et al., 2015). Animals expressing soluble GFP under the CX3CR1 promoter (resident macrophages) and the soluble red fluorescent protein under the CCR2 promoter (recruited macrophages) were obtained by crossing CX3CR1gfp/gfp and CCR2rfp/rfp (Mizutani et al., 2012). The prostates were imaged at Day 3 after surgery in sham-castrated or castrated mice.

2.9 | Statistics

Results are presented as the mean \pm standard deviation of the mean. analysis of variance and Tukey's post hoc testing were used for the comparison between experimental groups. Statistical significance was obtained when $p < 0.05$.

3 | RESULTS

Mining DNA microarray results by Desai et al. (2004) for genes transiently expressed after castration revealed an on-off pattern of *Zfn142* expression, with the on-phase at 72 hr after castration (Figure 1a). Immunohistochemistry identified ZNF142-positive cells scattered in the epithelial layer in castrated, but not in sham-castrated animals (Figure 1b), and the same cells were CD68-positive macrophages (ED1; Figure 1c). In spite of the proposed transcription regulation function, ZNF142 was found in discrete areas in the cytoplasm, close to CD68-positive areas, but in distinct domains within the same cell. To demonstrate that macrophages are recruited to the prostate after castration, we used intravital confocal microscopy (Marques et al., 2015) to examine the presence of resident CX3CR1-positive and recruited CCR2-positive cells in the gland in noncastrated, sham-operated, and castrated mice. CX3CR1+ cells showed no significant changes, while the CCR2+ cells accumulated in the gland (Figure 2a).

Earlier attempts to identify the M1 (iNOS-positive) and M2 (arginase- and mannose receptor-positive) phenotypes showed that both cell types are restricted to the stroma and absent from the epithelial layer. However, a day-by-day characterization of these phenotypes confirmed that M2-macrophages were not found in the epithelium, but revealed the presence of iNOS-positive, M1-polarized macrophages at Day 3 after castration (Figure 2b). However, M1 was found within the epithelial layer neither in sham-operated, noncastrated animals nor in castrated animals 5 days after surgery, reproducing the on-off pattern of *Znf142* expression. Given the

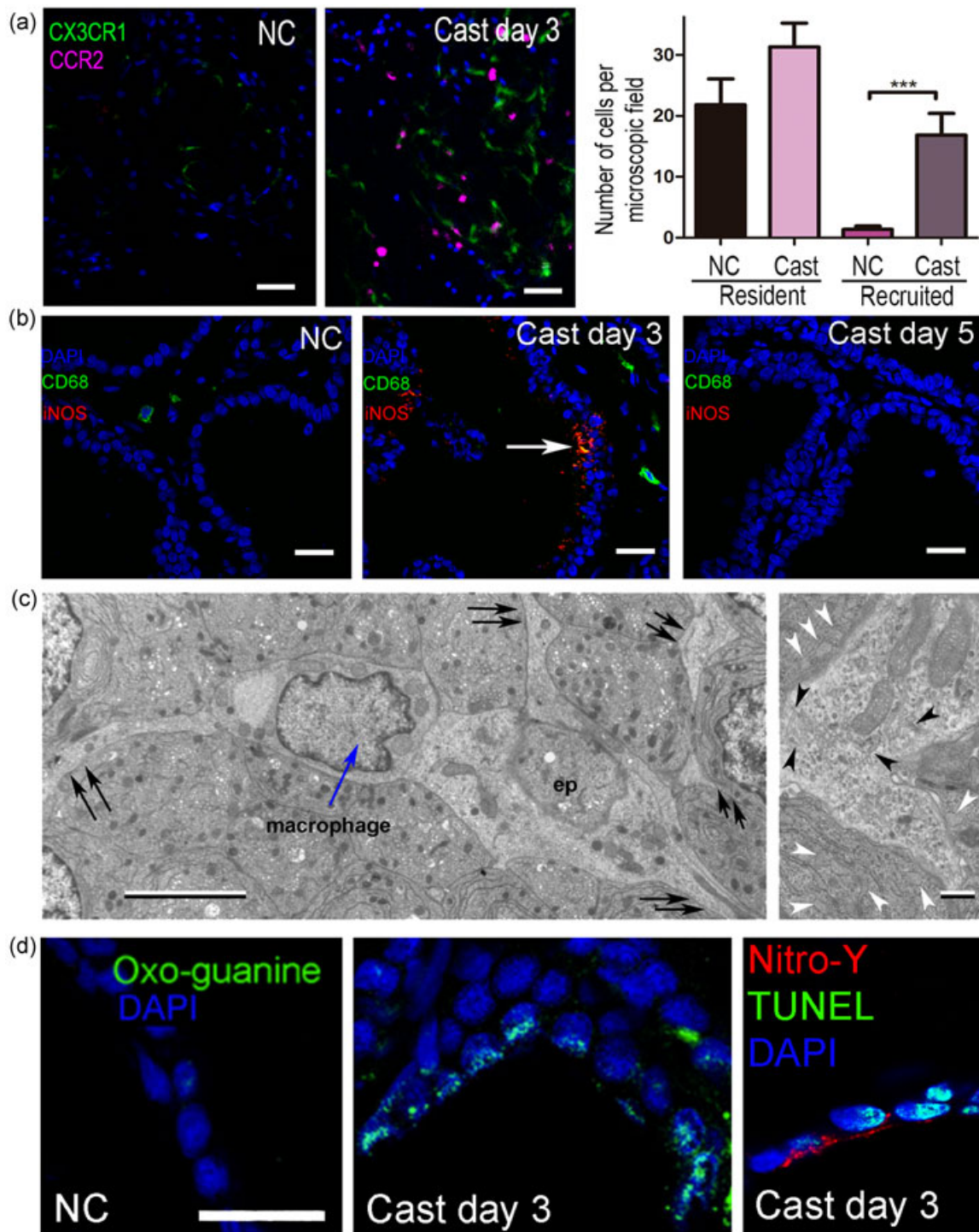


FIGURE 2 M1-macrophage polarization causes oxidative stress in epithelial cells. (a) Intravital microscopy revealed the presence of resident CX3CR1^{gfp+} macrophages in the sham-operated, noncastrated control, and the accumulation of recruited CCR2^{gfp+} macrophages in the glands at Day 3 after castration. Scale bars = 80 μ m (left panel) and 120 μ m (middle and right panels; $n = 3$, 10 microscopic fields per animal). (b) M1-macrophages expressing iNOS (white arrow) were found in the epithelial layer 3 days after castration but neither in sham-operated noncastrated controls nor in the prostate of rats castrated 5 days before. Scale bars = 25 μ m. (c) At the ultrastructural level, the M1-macrophages showed long, slender cell processes (double arrows) extending among the epithelial cells and in intimate contact with them. Higher magnification of one such cell process revealed the presence of varicose tubules (black arrowheads), glycogen granules and mitochondria. Adjacent epithelial cells showed enlarged ER cisterns (white arrowheads). Scale bars = 5 μ m and 0.5 μ m, respectively. (d) Immunocytochemistry revealed the presence of 8-oxoguanine and nitrosylated-tyrosine in the epithelial cells on Day 3 after castration but not in the control rat. TUNEL reaction revealed the presence of DNA double-strand breaks in cells lacking the morphological aspects of apoptosis. Scale bars = 20 μ m. 8-oxoguanine: 8-oxo-7,8-dihydroguanine; TUNEL: terminal deoxynucleotidyl transferase dUTP nick end labeling [Color figure can be viewed at wileyonlinelibrary.com]

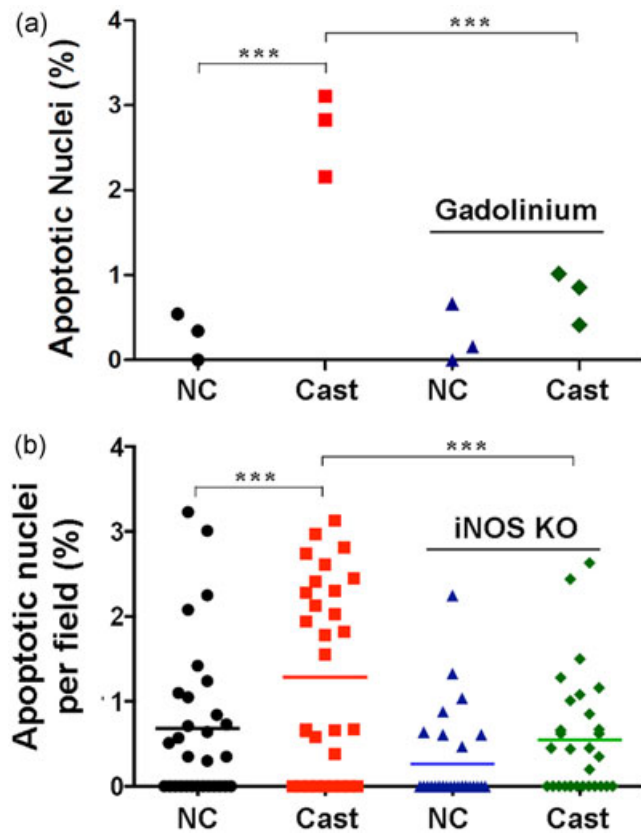


FIGURE 3 Macrophages and iNOS are implicated in epithelial cell apoptosis. (a) Depletion of macrophages with gadolinium chloride before castration resulted in a significant decrease in the percentage of apoptotic nuclei at Day 3 after castration (each data point is the mean number of apoptotic cells per animal; $p < 0.001$, asterisks; ANOVA and Tukey's post hoc tests, $n = 3$). (b) Lack of iNOS in the *Nos2* knockout mouse resulted in a significant decrease in the number of apoptotic cells in prostate gland at Day 3 after castration (each data point is the percentage of apoptotic cells per microscopic field counted in three animals; $p < 0.001$, asterisks; ANOVA and Tukey's post hoc tests, $n = 3$). ANOVA: analysis of variance [Color figure can be viewed at wileyonlinelibrary.com]

coincident expression of *Znf142* in CD68⁺ macrophages and the timing of M1-polarization, we named these CD68⁺/iNOS⁺/ZNF142⁺ cells M1₁₄₂-macrophages.

We used transmission electron microscopy to examine candidate M1₁₄₂-macrophages (differing from those engulfing epithelial cell corpses and previously characterized as expressing autophagy antigens in association with phagocytosis; Silva et al., 2017) and identified cells with slender processes and intimate contact with the epithelial cells. These cell processes were filled with varicose tubes in association with abundant glycogen granules and few mitochondria (Figure 2c). These aspects might be related to the respiratory burst need to provide high energy to produce nitric oxide (NO) and oxygen species. Adjacent epithelial cells showed signs of stress, such as dilated ER cisternae (Figure 2c, right panel).

M1-macrophages (and other phagocytes) express NADPH-oxidase, whose product is superoxide anion (O_2^-). Spontaneous processing of O_2^- in low pH (typical of endocytic vacuoles) or by the enzyme

superoxide dismutase, results in hydrogen peroxide and other reactive oxygen species (ROS), which react with NO to form the extremely reactive peroxynitrite. Exposure of DNA to these oxidative species results in DNA-DSB and 8-oxo-7,8-dihydroguanine (8-oxoguanine). Thus, we searched for these two types of DNA damage. Immunohistochemistry using an anti-8-oxoguanine antibody showed the presence of 8-oxoguanine in the nuclei of epithelial cells at Day 3 after castration, but not in the sham-operated, noncastrated control (Figure 2d). In addition, we used the TUNEL reaction and found focal points of DNA-DSB in the nuclei of epithelial cells (Figure 2d, right panel). Considering that peroxynitrite reacts with proteins to produce nitrosylated amino acid residues (Htet Hlaing & Clément, 2014), we investigated whether nitrotyrosine could be detected by immunohistochemistry and, accordingly, found immune-reactivity for nitrotyrosine in the epithelial cells, which showed focal labeling by the TUNEL reaction (Figure 2d, right panel). In addition, labeling was focal i.e. affected several cells in small areas.

These results associate focal DNA-DSB and oxidative stress, which was revealed by the presence of 8-oxoguanine and nitrotyrosine. They also demonstrate that the M1₁₄₂-macrophages are associated with epithelial cell apoptosis and that their interaction with epithelial cells results in cellular stress, including focal DNA damage.

The striking time and space association between the on-phase of *Znf142* expression in CD68⁺ macrophages and the peak of epithelial cell apoptosis (Damas-Souza et al., 2010; English et al., 1989; Isaacs, 1984; Kyprianou & Isaacs, 1988) led us to hypothesize that the latter could be causally linked to epithelial cell death. To test this hypothesis, we treated rats with gadolinium chloride (Liou et al., 2013) to deplete macrophages before castration and counted the number of apoptotic cells on Day 3 after surgery. The treatment was effective as shown by immunohistochemistry for ED1 macrophages (Silva et al., 2018). The results showed a significant reduction in the percentage of apoptotic cells (Figure 3a), confirming that the presence of macrophages was necessary for epithelial cell death. To determine whether M1-polarization (and hence, iNOS expression) was necessary for epithelial cell apoptosis, we counted the number of apoptotic epithelial cells in the ventral prostate of iNOS (*Nos2*) KO mice castrated 3 days before. Consistently, the iNOS KO mouse had significantly fewer apoptotic cells (Figure 3b), suggesting that expression of the enzyme iNOS (characterizing the M1-phenotype) was also causally linked to prostate epithelial cell apoptosis 72 hr after castration. Several microscopic fields were void of apoptotic cells, again suggesting that the apoptotic response is localized, instead of systemic.

To further characterize the interaction between macrophages and prostate epithelial cells, we performed cocultures of mouse prostate epithelial cells isolated by trypsin digestion and fractionation in Percoll gradient, and M1-macrophages differentiated in vitro after LPS and interferon-gamma stimulation. Surprisingly, under these conditions, the M1-macrophages died swiftly after contacting the epithelial cell layer both in the presence and absence of 1 nM DHT. Then, we cocultured isolated epithelial cells and undifferentiated mononuclear

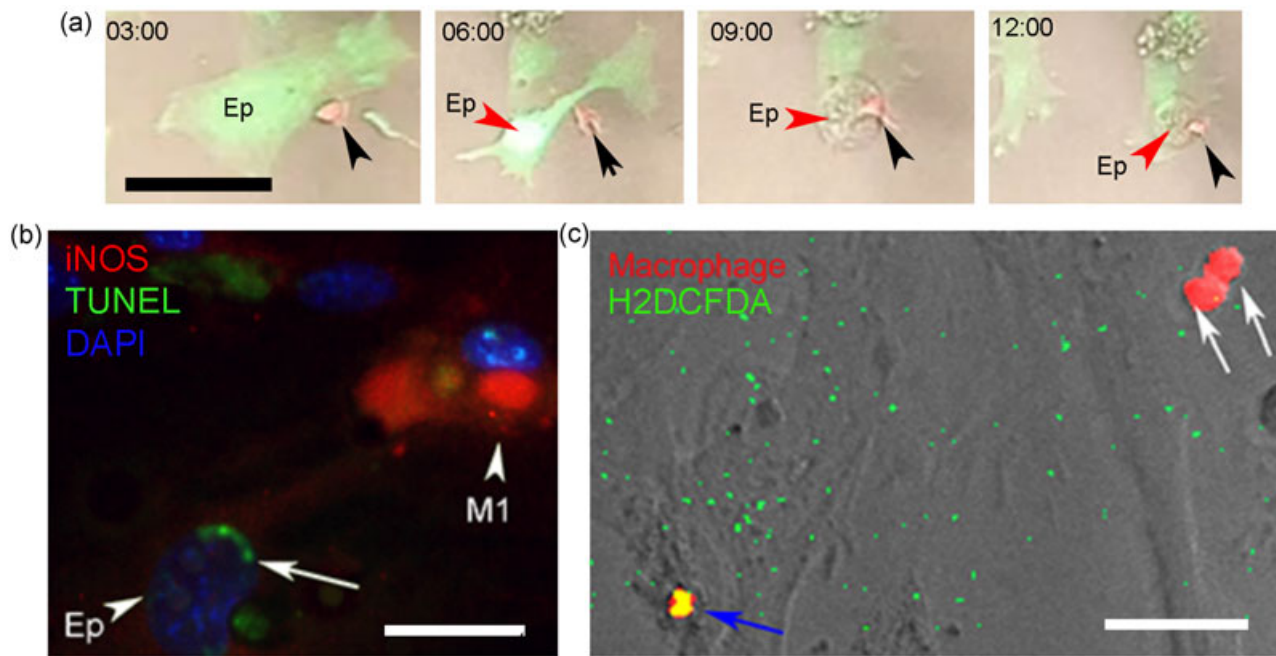


FIGURE 4 M1-macrophages differentiated in cocultures with epithelial cells causes oxidative stress and epithelial cell death. (a) Coculture of primary epithelial cells (Ep, green, red arrowheads) from the GFP-mouse and UMNC (red, black arrowheads) from the DsRed-mouse, revealed attacks of the former by the latter, leading to apoptosis of the epithelial cells within 9 hr of observation. Scale bars = 25 μ m. See also supplementary video. (b) Immunocytochemistry for iNOS and TUNEL reaction showed that macrophages are M1-polarized (red) and that their interaction with the epithelial cells caused focal areas of DNA double-strand breaks in the epithelial cells (green, white arrow). Scale bars = 5 μ m. (c) Primary cells from wild-type mouse loaded with the H2DCFDA probe showed activation of the probe (blue arrow) when in contact with primary macrophages isolated from the DsRed-mouse (white arrows), resulting in the orange color. The image is a snapshot from a movie made with the binary version of the original RGB frames. Scale bars = 10 μ m. GFP: green fluorescent protein; UMNC: undifferentiated mononuclear cells [Color figure can be viewed at wileyonlinelibrary.com]

cells (UMNCs) isolated from the bone marrow and found that the macrophage precursors interacted with the epithelial cell layer. To better observe the behavior of each cell type in culture, we repeated the above experiment, using epithelial cells isolated from the actin promoter-regulated soluble GFP transgenic mice, and macrophage precursors from the ubiquitin-promoter regulated soluble DS-red transgenic mice. It became clear that macrophages actively chased epithelial cells, which undergo apoptosis (Figure 4a, Movie 1). The macrophage precursors differentiated into the iNOS-positive, M1-macrophages in the absence of DHT (Figure 4b). Remarkably, the labeling for iNOS used to phenotype the M1-polarized macrophages revealed a network of interconnected tubules (Figure 5a), which were similar to those observed by electron microscopy (Figure 2c). In addition, we noticed that the epithelial cells in coculture with macrophage precursors in the absence of DHT showed foci of DNA-DSB (revealed by TUNEL; Figure 4b), similar to what was found *in vivo*. To dissect whether these DSB resulted from oxidative stress, we loaded wild-type epithelial cells with the oxidative stress probe H2DCFDA and cocultured them with DS-red macrophages in the absence of DHT. The results showed H2DCFDA activation inside the epithelial cells upon cell-cell interaction with the macrophages (Figure 4c).

Furthermore, we could differentiate M1-macrophages *in vitro* upon treatment of UMNC with the conditioned medium obtained by

culturing epithelial cells in the absence of DHT, suggesting that soluble factors are responsible for the differentiation of macrophage precursors. In contrast, in the presence of DHT, the UMNC interacted with the epithelial cell layer and adopted a scavenging behavior before dying. Using CD8 markers and flow cytometry, we excluded the possibility of having T-cytotoxic lymphocytes in our preparations (results not shown).

Finally, we tested whether the same phenomena could be reproduced with cell lineages, using the human androgen-responsive LNCaP cells and the mouse Raw 264.7 macrophages. First, we found that Raw 264.7 cells expressed either iNOS (M1-phenotype) or arginase (M2-phenotype) after treatment with LPS or IL-4, respectively (not shown). Then we treated Raw 264.7 cells with the LNCaP conditioned medium (10% in the macrophage culture medium) and noticed that it was capable to induce the differentiation of the M1-phenotype, in the absence of R1881 (Figure 5a,b). In the presence of R1881, we obtained arginase-expression, suggesting the M2-phenotype (not shown). Then we cocultured LNCaP and Raw 264.7 cells either in the presence or absence of R1881. In the absence of androgen stimulation, we found an increased frequency of TUNEL and cleaved caspase-9 double-positive cells (Figure 5c,d), but not cleaved caspase-8 (not shown), suggesting activation of the intrinsic apoptotic pathway. The M1-polarized macrophages were also ZNF142-positive (not shown).

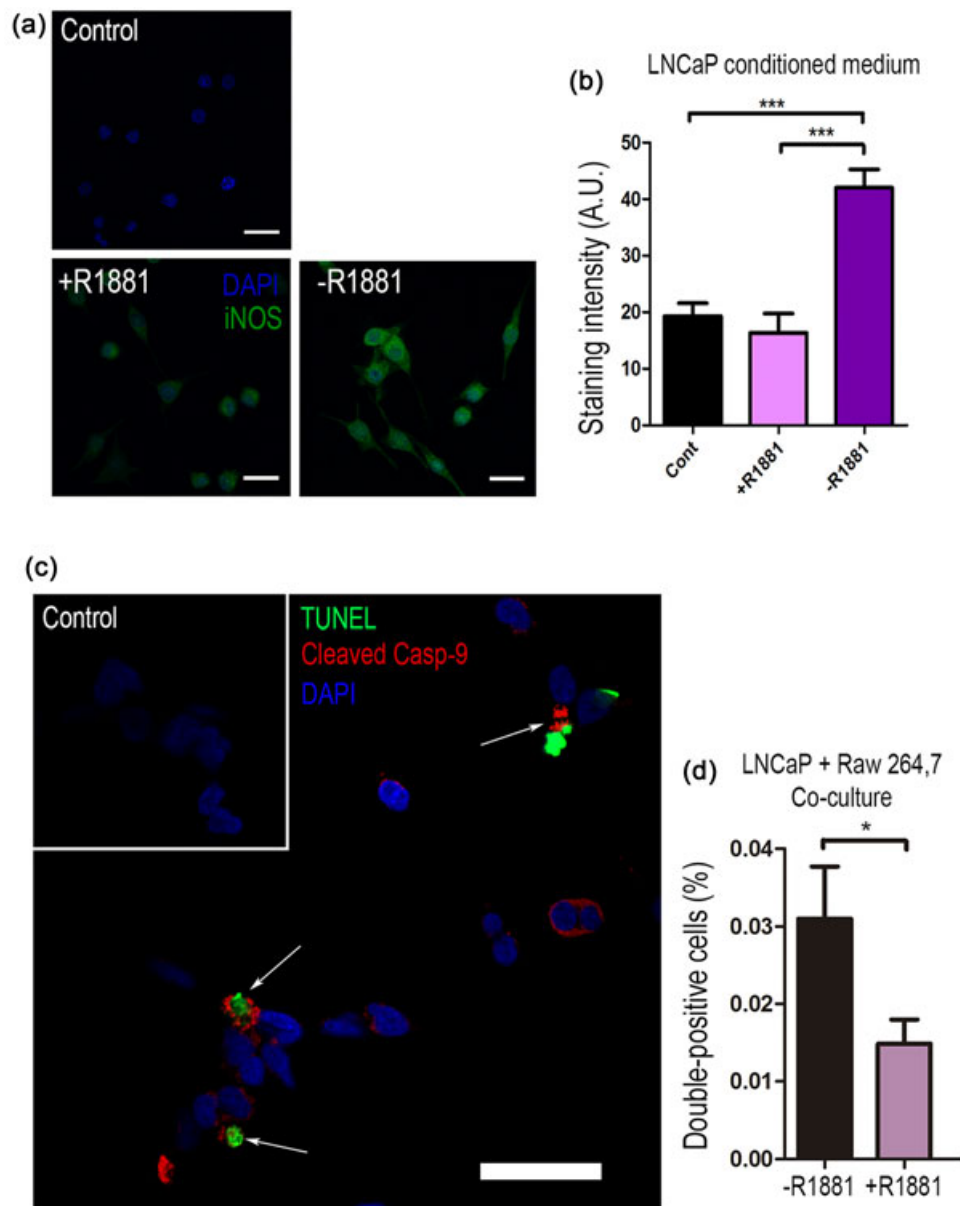


FIGURE 5 LNCaP cultured medium affects Raw 264.7 cells polarization and the M1-polarized cells promote epithelial cell death. (a) The LNCaP conditioned medium in the absence of R1881 resulted in M1-polarization (iNOS expression). (b) Quantification of iNOS-staining intensity in a per cell basis. (c) LNCaP and Raw 264.7 cocultures in the absence of R1881 resulted in an increased frequency of TUNEL (DNA-fragmentation) and cleaved (active) caspase-9 double-positive cells, suggesting activation of the intrinsic apoptotic pathway. Controls in (a) and (c) are the negative controls for the immunocytochemistry after exposure to the conditioned medium. Scale bars = 20 μ m. ANOVA (b) and Student's t-test (d) were used. ANOVA: analysis of variance; TUNEL: terminal deoxynucleotidyl transferase dUTP nick end labeling [Color figure can be viewed at wileyonlinelibrary.com]

4 | DISCUSSION

The data presented in this work show that prostate epithelial cells can induce macrophage polarization into M1₁₄₂ and that both cell types engage in cell-cell interactions. They also demonstrate that ROS are formed inside the epithelial cells at the sites of contact with the macrophages and multiple encounters results in epithelial cell apoptosis. The present observations suggest that (a) castration-induced epithelial cell death in the prostate gland is nonautonomous and relies on M1₁₄₂-macrophage polarization in response to epithelial cell-derived factors,

that (b) the activity of the M1₁₄₂-polarized macrophages includes the production of NO and superoxide (and their by-product peroxynitrite), which promote extensive DNA damage and other stresses, thereby resulting in the activation of the intrinsic apoptosis pathway and that (c) the same phenomenon can be reproduced using the androgen-responsive LNCaP human cells and Raw 264.7 mouse macrophages.

Macrophages have been implicated in endothelial cell apoptosis concurring with vascular remodeling (Diez-Roux & Lang, 1997), vascular smooth muscle cell death in vitro (Boyle, Weissberg, & Bennett, 2002), and control endotrophoblastic invasion (Reister

et al., 2001). Both NO and TNF-R have been implicated in these interactions. However, none of these studies have implied a direct attack based on an oxidative stress arsenal, promoting DNA damage and activation of the intrinsic apoptosis pathway.

Previously, we have demonstrated the presence of sequential waves of apoptosis after castration and the existence of a metalloprotease-dependent peak of apoptosis at Day 11 after surgery (Bruni-Cardoso, Augusto, Pravatta, Damas-Souza, & Carvalho, 2010). The mechanism proposed herein might be particular to the peak of apoptosis taking place at Day 3 post castration, given that no macrophages were found at Day 11. The proposed mechanism is also consistent with the fact that apoptotic cells are found in clusters, rather than being isotropically distributed in the epithelial layer, as expected from a systemic endocrine-regulation. The TNF/TNF-R pathway (Davis et al., 2011) has not been included in our analysis and hence cannot be excluded from the mechanism leading to epithelial cell death proposed here.

ZNF142 is a zinc finger protein with a putative function in transcription regulation. It occupies discrete regions in the cytoplasm of CD68-positive macrophages. ZNF142 might be important either for the transient nature of *Nos2* (and other M1 markers) expression or for the short life span of the polarized macrophages within the time window corresponding to the 3rd day after castration, but this will need further investigation.

In this study, we have designed the experiments to avoid exposure of macrophages to androgens and to restrict their behavior as a response to soluble factors produced by epithelial cells. Given that macrophages express the androgen receptor and thus are responsive to androgens (Lai et al., 2009), this issue will need further research in the future and is certainly a fragility of the present work.

Careful analysis of the results presented here led us to suggest that a binary die-survive pattern might exist *in vivo*, i.e., the M1₁₄₂-interaction with a particular epithelial cell will proceed until the intrinsic apoptotic pathway is triggered and the epithelial cell dies. This occurs essentially because epithelial cells are sessile, due to cell-cell and cell-basement membrane adhesions. In culture, the encounters of macrophage and epithelial cells are less effective and multiple interactions are needed to induce epithelial cell death because the epithelial cells are mobile and migrate away from macrophages. Nonetheless, we also believe that this binary die-survive mechanism might be subverted in situations where macrophage effectiveness is compromised, such as in inflammatory states and/or when targeting cancer cells. Confronting inflammatory mediators and/or increased mobility of the cancer cells are putative factors affecting macrophage effectiveness to induce epithelial cell apoptosis. Moreover, intrinsic changes in resident and newly-induced M1₁₄₂-macrophages characterizing immunometabolism (Oishi & Manabe, 2015) and immunosenescence (Aw, Silva, & Palmer, 2007; Gruver, Hudson, & Sempowski, 2007), which affects the balance between lymphoid and myeloid cells and macrophage function, must be considered, as they contribute to the differences between the physiology in experimental young adult animals and that taking place in mature men experiencing antiprostata cancer therapies.

Recent studies have contributed to the rapid accumulation of information, demonstrating that CRPC behavior cannot be explained solely by changes in the cells' ability to survive and to proliferate under low androgen conditions. Recently, NEK6 has been implicated in the ability of CRPC cells to survive (Atish et al., 2017). Sequencing and lineage tracing has proven that metastatic prostate cancer does not necessarily arise from the most advanced localized tumors (Cooper et al., 2015; Haffner et al., 2013; Van Etten & Dehm, 2016). Systematic sequencing has also revealed that advanced CRPC cells have extensive chromosomal translocation and bridges, which were collectively designated chromoplexy (Baca et al., 2013). Both types of evidence point to the possibility that prostate cancer progression has punctate, nonlinear features (Baca et al., 2013), contrasting with the step-wise and progressive acquisition of genomic, physiological and micro-environmental properties compatible with the transition from the normal to the nonmalignant to the malignant phenotypes in other cancer types.

In conclusion, we unveiled that the classical peak epithelial cell apoptosis occurring 72 hr after castration depends on interactions between epithelial cells and macrophages in the hypoandrogen environment. This includes unknown factors produced by the former and a respiratory burst in the latter to produce cell stress and focal DNA damage. We speculate that chromoplexy and other aspects of CRPC result from broken/interrupted macrophage-epithelial cell interactions, which would promote DNA damage, but not cell death. DSB repair, including nonhomologous end joining, and alternative repair pathways due to the presence of 8-oxoguanine (Fortini et al., 2003), would lead to the multiple chromosome translocations and bridges typical of chromoplexy and increased genomic instability, generating the cellular variability for selection of CRPC cells, including the capacity to survive and proliferate in the hypoandrogen environment.

ACKNOWLEDGMENTS

We thank Dr. J. Xavier Neto for providing the DS-red mice and Dr. Mario J. Saad for the iNOS KO mice. This study was funded by FAPESP (grant 2009/016150-6) and CNPq. INFABiC is cofunded by FAPESP and CNPq.

CONFLICT OF INTERESTS

The authors declare that there is no conflict of interests.

AUTHOR CONTRIBUTIONS

Conception or design of the work (G. O. B., J. A. P. F. S., U. N., A. B. C., and H. F. C.). Acquisition, analysis, or interpretation of data for the work (G. O. B., J. A. P. F. S., A. S. B., U. N., R. R. R., S. B. P. O., M. O. B., D. F., J. C. O. S., D. M. D. S., A. B. C., T. M. A., R. C. S., S. L. F., G. B. M., C. L. C., and H. F. C.). Drafting the work or revising it critically for important intellectual content (G. O. B., J. A. P. F. S., A. S. B., U. N., A. B. C., P. M. M. V., C. L. C., and H. F. C.).

ORCID

Hernandes F. Carvalho  <http://orcid.org/0000-0002-3080-9447>

REFERENCES

- Atish, D. C., Anna, C. S., Maura, B. C., Rosina, T. L., Katherine, L., Ying, J. L., ... William, C. H. (2017). Castration resistance in prostate cancer is mediated by the kinase NEK6. *Cancer Research*, *77*, 753–765.
- Aw, D., Silva, A. B., & Palmer, D. B. (2007). Immunosenescence: Emerging challenges for an ageing population. *Immunology*, *120*, 435–446.
- Baca, S. C., Prandi, D., Lawrence, M. S., Mosquera, J. M., Romanel, A., Drier, Y., ... Park, K. (2013). Punctuated evolution of prostate cancer genomes. *Cell*, *153*, 666–677.
- Boyle, J. J., Weissberg, P. L., & Bennett, M. R. (2002). Human macrophage-induced vascular smooth muscle cell apoptosis requires NO enhancement of Fas/Fas-L interactions. *Arteriosclerosis, Thrombosis, and Vascular Biology*, *22*, 1624–1630.
- Bruni-Cardoso, A., Augusto, T. M., Pravatta, H., Damas-Souza, D. M., & Carvalho, H. F. (2010). Stromal remodelling is required for progressive involution of the rat ventral prostate after castration: Identification of a matrix metalloproteinase-dependent apoptotic wave. *International Journal of Andrology*, *33*, 686–695.
- Carvalho, H. F., & Line, S. R. (1996). Basement membrane associated changes in the rat ventral prostate following castration. *Cell Biology International*, *20*, 809–819.
- Cooper, C. S., Eeles, R., Wedge, D. C., Van Loo, P., Gundem, G., Alexandrov, L. B., ... Kremeyer, B. (2015). Analysis of the genetic phylogeny of multifocal prostate cancer identifies multiple independent clonal expansions in neoplastic and morphologically normal prostate tissue. *Nature Genetics*, *47*, 367–372.
- Damas-Souza, D. M., Oliveira, C. A., & Carvalho, H. F. (2010). Insulin affects tissue organization and the kinetics of epithelial cell death in the rat ventral prostate after castration. *Journal of Andrology*, *31*, 631–640.
- Davis, J. S., Nastiuk, K. L., & Krolewski, J. J. (2011). TNF is necessary for castration-induced prostate regression, whereas TRAIL and FasL are dispensable. *Molecular Endocrinology*, *25*, 611–620.
- Desai, K. V., Michalowska, A. M., Kondaiah, P., Ward, J. M., Shih, J. H., & Green, J. E. (2004). Gene expression profiling identifies a unique androgen-mediated inflammatory/immune signature and a PTEN (phosphatase and tensin homolog deleted on chromosome 10)-mediated apoptotic response specific to the rat ventral prostate. *Molecular Endocrinology*, *18*, 2895–2907.
- Diez-Roux, G., & Lang, R. A. (1997). Macrophages induce apoptosis in normal cells in vivo. *Development*, *124*, 3633–3638.
- English, H. F., Kyprianou, N., & Isaacs, J. T. (1989). Relationship between DNA fragmentation and apoptosis in the programmed cell death in the rat prostate following castration. *Prostate (New York, NY)*, *15*, 233–250.
- Feldman, B. J., & Feldman, D. (2001). The development of androgen-independent prostate cancer. *Nature Reviews Cancer*, *1*, 34–45.
- Fortini, P., Pascucci, B., Parlanti, E., D'Errico, M., Simonelli, V., & Dogliotti, E. (2003). 8-Oxoguanine DNA damage: At the crossroad of alternative repair pathways. *Mutation Research*, *531*, 127–139.
- Gruver, A. L., Hudson, L. L., & Sempowski, G. D. (2007). Immunosenescence of ageing. *Journal of Pathology*, *211*, 144–156.
- Haffner, M. C., Mosbrugger, T., Esopi, D. M., Fedor, H., Heaphy, C. M., Walker, D. A., ... Yegnasubramanian, S. (2013). Tracking the clonal origin of lethal prostate cancer. *Journal of Clinical Investigation*, *123*, 4918–4922.
- Heinlein, C. A., & Chang, C. (2004). Androgen receptor in prostate cancer. *Endocrine Reviews*, *25*, 276–308.
- Htet Hlaing, K., & Clément, M.-V. (2014). Formation of protein S-nitrosylation by reactive oxygen species. *Free Radical Research*, *48*, 996–1010.
- Isaacs, J. T. (1984). Antagonistic effect of androgen on prostatic cell death. *Prostate (New York, NY)*, *5*, 545–557.
- Kashiwagi, B., Shibata, Y., Ono, Y., Suzuki, R., Honma, S., & Suzuki, K. (2005). Changes in testosterone and dihydrotestosterone levels in male rat accessory sex organs, serum, and seminal fluid after castration: Establishment of a new highly sensitive simultaneous androgen measurement method. *Journal of Andrology*, *26*, 586–591.
- Kerr, J. F., & Searle, J. (1973). Deletion of cells by apoptosis during castration-induced involution of the rat prostate. *Virchows Archive B: Cell Pathology*, *13*, 87–102.
- Kurita, T., Wang, Y. Z., Donjacour, A. A., Zhao, C., Lydon, J. P., O'Malley, B. W., ... Cunha, G. R. (2001). Paracrine regulation of apoptosis by steroid hormones in the male and female reproductive system. *Cell Death and Differentiation*, *8*, 192–200.
- Kyprianou, N., & Isaacs, J. T. (1988). Activation of programmed cell death in the rat ventral prostate after castration. *Endocrinology*, *122*, 552–562.
- Lai, J. J., Lai, K. P., Chuang, K. H., Cang, P., YU, I. C., Lin, W. J., & Chang, C. (2009). Monocyte/macrophage androgen receptor suppresses cutaneous wound healing in mice by enhancing local TNF-alpha expression. *Journal of Clinical Investigation*, *119*, 3739–3751.
- Liou, G. Y., Döppler, H., Necela, B., Krishna, M., Crawford, H. C., Raimondo, M., & Storz, P. (2013). Macrophage-secreted cytokines drive pancreatic acinar-to-ductal metaplasia through NF-KB and MMPs. *Journal of Cell Biology*, *202*, 563–577.
- Marques, P. E., Antunes, M. M., David, B. A., Pereira, R. V., Teixeira, M. M., & Menezes, G. B. (2015). Imaging liver biology in vivo using conventional confocal microscopy. *Nature Protocols*, *10*, 258–268.
- McPherson, S. J., Hussain, S., Balanathan, P., Hedwards, S. L., Niranjani, B., Grant, M., ... Risbridger, G. P. (2010). Estrogen receptor-beta activated apoptosis in benign hyperplasia and cancer of the prostate is androgen independent and TNFalpha mediated. *Proceedings of the National Academy of Sciences of the United States of America*, *107*, 3123–3128.
- Mizutani, M., Pino, P. A., Saederup, N., Charo, I. F., Ransohoff, R. M., & Cardona, A. E. (2012). The fractalkine receptor but not CCR2 is present on microglia from embryonic development throughout adulthood. *Journal of Immunology*, *188*, 29–36.
- Oishi, Y., & Manabe, I. (2015). Immunometabolic control of homeostasis and inflammation. *Inflammation and Regeneration*, *35*, 185–192.
- Powell, W. C., Fingleton, B., Wilson, C. L., Boothby, M., & Matrisian, L. M. (1999). The metalloproteinase matrilysin proteolytically generates active soluble Fas ligand and potentiates epithelial cell apoptosis. *Current Biology*, *9*, 1441–1447.
- Reister, F., Frank, H. G., Kingdom, J. C., Heyl, W., Kaufmann, P., Rath, W., & Huppertz, B. (2001). Macrophage-induced apoptosis limits endovascular trophoblast invasion in the uterine wall of preeclamptic women. *Laboratory Investigation*, *81*, 1143–1152.
- Rosa-Ribeiro, R., Barbosa, G. O., Kühne, F., & Carvalho, H. F. (2014). Desquamation is a novel phenomenon for collective prostate epithelial cell deletion after castration. *Histochemistry and Cell Biology*, *141*, 213–220.
- Rosa-Ribeiro, R., Nishan, U., Vidal, R. O., Barbosa, G. O., Reis, L. O., Cesar, C. L., ... Carvalho, H. F. (2014). Transcription factors involved in prostate gland adaptation to androgen deprivation. *PLoS One*, *9*, e97080.
- Shabsigh, A., Chang, D. T., Heitjan, D. F., Kiss, A., Olsson, C. A., Puchner, P. J., & Buttyan, R. (1998). Rapid reduction in blood flow to the rat ventral prostate gland after castration: Preliminary evidence that androgens influence prostate size by regulating blood flow to the prostate gland and prostatic endothelial cell survival. *Prostate (New York, NY)*, *36*, 201–206.
- Silva, J. A. F., Bruni-Cardoso, A., Augusto, T. M., Damas-Souza, D. M., Barbosa, G. O., Felisbino, S. L., ... Carvalho, H. F. (2018). Macrophage roles in the clearance of apoptotic cells and control of inflammation in the prostate gland after castration. *Prostate (New York, NY)*, *78*, 4–9.
- Sugihara, A., Yamada, N., Tsujimura, T., Iwasaki, T., Yamashita, K., Takagi, Y., ... Terada, N. (2001). Castration induces apoptosis in the male accessory sex organs of Fas-deficient lpr and Fas ligand-deficient gld mutant mice. *In Vivo (Brooklyn)*, *15*, 385–390.
- Tommerup, N., & Vissing, H. (1995). Isolation and fine mapping of 16 novel human zinc finger-encoding cDNAs identify putative

candidate genes for developmental and malignant disorders. *Genomis*, 27, 259–264.

Van Etten, J. L., & Dehm, S. M. (2016). Clonal origin and spread of metastatic prostate cancer. *Endocrine-Related Cancer*, 23, R207–R217.

SUPPORTING INFORMATION

Additional supporting information may be found online in the Supporting Information section at the end of the article.

How to cite this article: Barbosa GO, Silva JAF, Siqueira-Berti A, et al. Castration-induced prostate epithelial cell apoptosis results from targeted oxidative stress attack of M1₁₄₂-macrophages. *J Cell Physiol*. 2019;1–11.

<https://doi.org/10.1002/jcp.28544>